JOURNAL OF Applied Polymer SCIENCE

Effect of Block Composition, Size and Functionality of Poly (Styrene-Isobutylene-Styrene) Copolymers

David Suleiman, Gretselle Carreras, Yahaira Soto
Department of Chemical Engineering, University of Puerto Rico, Mayagüez, Puerto Rico 00681-9000
Correspondence to: D. Suleiman (E-mail: David.Suleiman@upr.edu)

ABSTRACT: This investigation studied the resulting nanostructure and transport properties of ionic membranes composed of sulfonated copolymers with thermoplastic and elastomeric blocks. Poly(styrene-isobutylene-styrene) (SIBS) of different number average molecular weight (M_n) and polystyrene weight fraction were sulfonated to various levels of ion exchange capacity. The solvent-casted membranes were characterized using several techniques including elemental analysis, Fourier transform infrared spectroscopy-, thermogravimetric analysis, and small-angle X-ray scattering. These techniques were used to evaluate the thermal and physical properties of the membranes, which in turn, allowed for the comparison of resulting morphologies and selectivities. In addition, counter-ion substitution (Mg^{+2}, Ca^{+2}, Ba^{+2}) was used to crosslink the sulfonated polymers to further influence their selectivity. Vapor permeabilities were measured at 308 K using dimethyl methyl-phosphonate, a chemical compound similar to Sarin Gas, and water, to evaluate the selectivity of the membranes and their potential application for chemical and biological protective clothing. © 2012 Wiley Periodicals, Inc. J. Appl. Polym. Sci. 000: 000–000, 2012

KEYWORDS: poly(styrene-isobutylene-styrene); block copolymer ionomers; selectivity; cation-substituted membranes; chemical and biological protective clothing

Received 9 February 2012; revised 9 May 2012; accepted 1 June 2012; published online
DOI: 10.1002/app.38154

INTRODUCTION

Protective clothing (PC) materials are used to selectively reduce the transport of chemicals and biological toxins while allowing air and water transport through a breathable material.[1,2] Block copolymer ionomers composed of elastomeric blocks with excellent barrier properties (e.g., polyisoprene, polybutadiene, and polyisobutylene) and glassy segments [e.g., polystyrene (PS)] that can be functionalized to create ionic nanochannels[3,4] have been considered attractive candidates for PC applications. Some of the key properties that make them useful for these applications are low cost and weight, high water and air permeability, high selectivity, and the ability to adhere to a variety of textile substrates. These polymers also create a highly interconnected ionic nanostructure on sulfonation and parameters such as morphology and the size of the ionic nanochannels can be controlled with the level of sulfonation.[4,5] Some of the block copolymer ionomers that have been evaluated in the past are as follows: sulfonated aromatic hydrocarbons,[3–8] polyether ketones,[9–11] polyether sulfones,[12,13] polyimides,[14–17] and a combination of elastomeric blocks with polymer ionic liquids.[18,19] Previous studies have shown significant variations in their selectivity as a result of differences in chemical blocks and morphology (e.g., linear vs. branched),[6] which play a critical role in the transport mechanism through the polymer membrane. In addition, the incorporation of organic and inorganic additives such as metallic cations,[20] SiO_2 nanoparticles,[21,22] and TiO_2 nanoparticles[23,24] has also been reported to influence the selectivity.

Block copolymer ionomers are also used in direct methanol fuel cells (DMFC). In DMFC, although protons are transported from the anode to the cathode through the proton exchange membrane (PEM), methanol is not selectively blocked and thus creates a problem known as the cross-over limitation. Many approaches have been tried to create polymer architectures (chemical and morphological) capable of selectively allowing protons through the PEM while blocking the methanol or any other fuel considered. Some of the block copolymers considered for DMFC could also be evaluated for PC applications, but it is important to emphasize that the transport mechanism might be unique for each permeant studied.

In this study, poly(styrene-isobutylene-styrene) (SIBS) with different average number molecular weight (M_n) and PS weight fraction were evaluated for potential PC applications. The different block copolymers were studied as a function of sulfonation level and counter-ion substitution (Ba^{+2}, Ca^{+2}, and Mg^{+2}) to understand if differences in physical properties could

influence the transport properties. Decreasing the PS weight fraction (increasing the % PIB) could potentially enhance the barrier properties and reduce the overall sites available for sulfonation, which could, in turn, influence the transport mechanism and the selectivity of the polymer membranes. In this study, a comprehensive materials characterization scheme was used to correlate the material nanostructure with the resulting transport properties.

EXPERIMENTAL

Materials

Poly(styrene-isobutylene-styrene) triblock copolymer was provided by Kuraray. Different grades were obtained: 22.5 wt % PS with a M_n = 65,000; 15 wt % PS with M_n = 100,000, and two different grades with 30 wt % PS, one with M_n = 65,000, and another with M_n = 100,000. Other chemicals used in this study include Toluene (Fisher Scientific, Optima*, 99.8%), Hexyl Alcohol (Aldrich, Reagent Grade, 98%), Methanol (Fisher Scientific, Optima*, 99.9%), Acetic Anhydride (Aldrich Chemical Company, 99+%), Sulfuric Acid (Sigma-Aldrich, 95–98%), Dimethyl Methyl-phosphonate (DMMP) (Aldrich, 97%), Magnesium Chloride (Sigma Aldrich, anhydrous, powder, 99.99%), Calcium Chloride (Sigma Aldrich, anhydrous, powder, 99.99%), Barium Chloride (Sigma Aldrich, anhydrous, powder, 99.99%), Water (Sigma-Aldrich, HPLC grade), and deionized water. All chemicals were used without further purification.

Sulfonation and Nomenclature

The sulfonation of SIBS was performed using the suggested procedure described elsewhere.[3] SIBS polymers are sulfonated in the para-position of the aromatic ring in the PS block of the polymer[3] (Figure 1). The sulfonation level of the polymer was controlled with the stoichiometric amount of the sulfonating agent (acetyl sulfate). The percent sulfonation (mole percent) corresponds to the available PS block in each polymer. Polymer membranes were labeled as SIBS-*W*-*X*-*Y*-*Z*, where *W* corresponds to the weight percent of PS in the block copolymer, *X* represents the number average molecular weight, *Y* is the sulfonation percent (mole fraction), and *Z* the substitution (acid or cation). For example, SIBS-30-65k-97-H corresponds to 30% PS, M_n = 65,000, 97% sulfonation of the membrane in its acidic form, whereas SIBS-15-100k-84-Ca corresponds to 15% PS, M_n = 100,000, 84% sulfonation of the calcium-substituted membrane. The amount of sulfonation was obtained after performing elemental analysis (EA), which was conducted by Atlantic Microlab, in Norcross, GA.

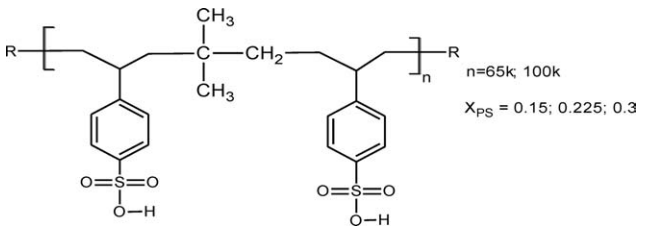

Figure 1. Chemical structure of sulfonated SIBS.

FourierTransform Infrared Spectroscopy

Fourier transform infrared (FTIR) spectroscopy was used to analyze chemical functional groups of organic compounds and to confirm identities with the peak positions and intensities. IR spectrums were collected in a Thermo Nicolet IR-300. A special ATR attachment was used for solid IR spectra. All IR spectra were collected using 64 scans and 4 cm^{-1} resolution.

Membrane Casting

Sulfonated polymers were dissolved in a solution of toluene/hexanol (85/15) (w/v) with a polymer concentration of 5% (w/v) and casted in an open Teflon® Petri dish using solvent casting at room temperature. The resulting membranes were casted as a consequence of thermodynamic self-assembly. Unsulfonated SIBS polymers were dissolved and casted using toluene with the same 5% polymer concentration.

Cation Substituted Cross-Linked Membranes

Counter-ion substitution was performed to influence the water swelling and selectivity of the resulting membranes. Cations attached to the sulfonic groups due to the chemical deficiency of ions in the electron shell of the polymer chain. The membranes were crosslinked by immersing them in a 1.0 M solution of $MgCl_2$, $CaCl_2$, and $BaCl_2$, depending on the desired cation for 24 h. They were then washed using deionized water and dried in an oven at approximately 60°C for several days.

To quantify the amount of cations substituted in the membranes, neutron activation analysis was used as an additional EA technique; these experiments were conducted by Elemental Analysis (Lexington, KY). The results (Table I) show three major findings: (1) Using a large excess (> 1000%) of the metal compared to the available sulfonic groups for 24 h allowed for consistent metal loading; different samples had the same results. (2) The molar ratio of metal to sulfonic groups was fairly constant regardless of sulfonation level for each of the +2 cations studied. (3) Although there were variations for the different metals studied, the average molar ratio of the metal to the sulfonic group was 0.47 ± 0.07 for all the +2 metals studied, suggesting that perhaps there is one cation for every two sulfonic groups. The individual averages show that Ca^{+2} (0.55 ± 0.06) was slightly higher than Mg^{+2} (0.48 ± 0.02), which was higher than Ba^{+2} (0.40 ± 0.03).

Thermogravimetric Analysis

A Mettler Toledo TGA/SDTA 851E was used to study the thermal degradation behavior of the membranes. Thermogravimetric analysis (TGA) was performed to determine changes in weight with respect to temperature. A membrane sample weighting approximately 5–6 mg was used for each experiment. Degradation temperatures were determined by heating the polymer samples in a nitrogen environment to 650°C at 10°C/min and observing regions of significant weight loss.

Small-Angle X-Ray Scattering

Small-angle X-ray scattering (SAXS) was performed on a beamline X27C to obtain information about the structure and morphology of the membranes. Two-dimensional scattering patterns were collected on a pinhole-collimated system using Fujitsu image plates and read by a Fujitsu BAS 200 image plate reader.

Table I. Metal Loadings from Elemental Analysis

Sample name	Mass (g)	Weight % S	Weight % metal	Moles of metal/moles of SO_3H
SIBS-30-65k-39-Mg^{+2}	0.103	3.5	1.3	0.49
SIBS-30-65k-63-Mg^{+2}	0.122	5.1	1.9	0.49
SIBS-30-65k-84-Mg^{+2}	0.119	5.6	2.1	0.49
SIBS-30-65k-83-Mg^{+2}	0.098	6.4	2.2	0.45
SIBS-30-65k-83-Mg^{+2}	0.098	6.3	2.2	0.46
				Average Mg^{+2} = 0.48 ± 0.02
SIBS-30-65k-39-Ca^{+2}	0.108	4.0	2.4	0.48
SIBS-30-65k-63-Ca^{+2}	0.119	4.8	3.4	0.57
SIBS-30-65k-84-Ca^{+2}	0.120	6.7	4.2	0.50
SIBS-30-65k-83-Ca^{+2}	0.095	5.9	4.1	0.56
SIBS-30-65k-83-Ca^{+2}	0.106	5.1	4.0	0.63
				Average Ca^{+2} = 0.55 ± 0.06
SIBS-30-65k-39-Ba^{+2}	0.102	3.6	6.5	0.42
SIBS-30-65k-63-Ba^{+2}	0.116	5.0	8.1	0.38
SIBS-30-65k-84-Ba^{+2}	0.105	6.3	9.7	0.36
SIBS-30-65k-83-Ba^{+2}	0.107	5.2	9.6	0.43
SIBS-30-65k-83-Ba^{+2}	0.107	5.6	9.4	0.39
				Average Ba^{+2} = 0.40 ± 0.03

The SAXSQuant software® was used to reduce two-dimensional data to one-dimensional intensity versus scattering vector (q) plots after background subtraction by circular averaging. The X-ray wavelength used was 1.6 Å. The calibration standard was silver behenate and the sample distance to the detector was 210 cm.

Water Swelling

Water-swelling measurements were performed using the immersion/gain method with membrane samples between 20 and 40 mg. The sample was initially dried at 70°C for 24 h in an oven (its original weight was recorded) and then, immersed in an excess amount of HPLC water solution (5 mL) at room temperature (23°C). The weight of the wet membranes was determined after different times until swelling equilibrium was reached. Each reported result represents the average of at least three repetitions. In this study, the effect of temperature on water swelling was not considered.

Vapor-Phase Permeability

Vapor-phase permeability experiments were conducted using an oven at 35°C with an inert atmosphere of nitrogen, an analytical balance (precision = 0.0001g) to measure weight loss, and 20 mL vials of open top caps with a 6 mm hole cut in the center of the Teflon septa, as shown in Figure 2. The membrane thickness was recorded prior to the experiment using a vernier caliper. Vials were filled with 5 mL of DMMP or 5 mL of water depending on the permeant analyzed and placed in the oven. Weight measurements were performed over a 1 week period of time. DMMP was selected as a simulant for the chemical toxin Sarin (nerve gas), due to its similarity in chemical structure, physical properties, and volatility (see Figure 3). Effective permeabilities (P_{eff}) [cm^2/s] were obtained from Fick's law (eq. 1):[25]

$$P_{\text{eff}} = \frac{L * \text{VTR}}{\left(P_i^{\text{vap}} \frac{\text{MW}_i}{RT}\right)} \quad (1)$$

where L is the thickness of the membrane [cm], P_i^{vap} is the vapor pressure of the permeant inside the vial [mmHg], R is the gas constant [cm^3 mmHg/mole K], T is the experiment temperature [K], MW_i is the permeant molecular weight (g/mole), and VTR the vapor transfer rate [g/s cm^2]. The VTR was

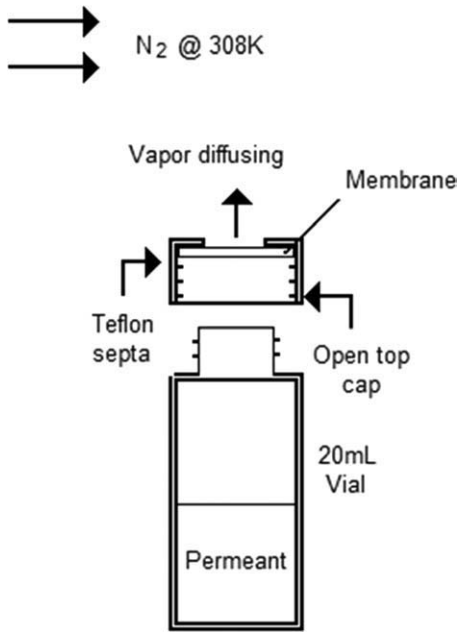

Figure 2. Schematic diagram for vapor-phase permeability experiments.

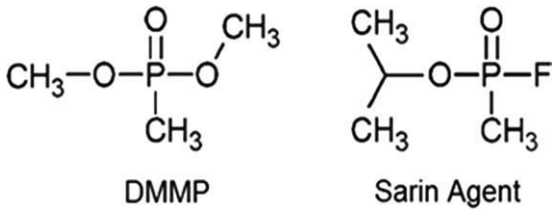

Figure 3. Chemical structures for DMMP and toxic agent Sarin.

obtained from the slope of the linear regression of the steady state part of the weight loss data vs. time, divided by the cross-sectional area for diffusion. The VTR divided by the molecular weight corresponds to the steady-state molar diffusion flux (J_i).

RESULTS AND DISCUSSION

FourierTransform Infrared Spectroscopy

Although EA was used to quantify the amount of sulfonation (mole %), FTIR spectroscopy was used to detect sulfonic groups in the polymers and the effect of the cation substitution in the crosslinked membranes. As shown in Figure 4, sulfonic groups appear in three different regions (marked with an asterisk, *) 1007, 1034, and 1126 cm^{-1}. Upon sulfonation, all polymers studied behaved similarly, regardless of M_n or % PS.

The interactions of the counter-ions with the sulfonic groups were evaluated comparing the sulfonic group peaks (Figure 5). On cation substitution, all polymers studied show a unique shift in the wavenumber toward higher energy, indicative of the strong and unique interaction for each cation with the sulfonic group peaks. Although each cation provokes a unique shift in each of the sulfonic groups, when evaluating the shift for each cation for the different polymers studied, one observes that each shift is the same regardless of polymer size (M_n) or block composition (% PS) (Figure 6).

Degradation Temperatures

Degradation temperature results are presented in Table II. All the unsulfonated polymers present only a single degradation temperature, corresponding to the polymer backbone. For the unsulfonated polymers, degradation temperatures increased with an increase in M_n but decreased with an increase in the % PS. Upon sulfonation, all the polymers studied show two degradation regions: the first weight loss stage can be attributed to the degradation of sulfonic groups and the second weight loss corresponds to the polymer backbone degradation. This behavior has been documented before for a single M_n and % PS.[26,27] For the sulfonated polymers, only one sulfonation is presented, as the degradation temperatures were the same regardless of sulfonation level. The first degradation temperature (sulfonic groups) is similar for all polymers studied except for SIBS-15-100k-80.7-H that showed a 13–21°C higher degradation temperature than the other polymers; however, the unsulfonated polymer (SIBS-15-100k-0-H) also showed a 10–46°C higher degradation temperature than the

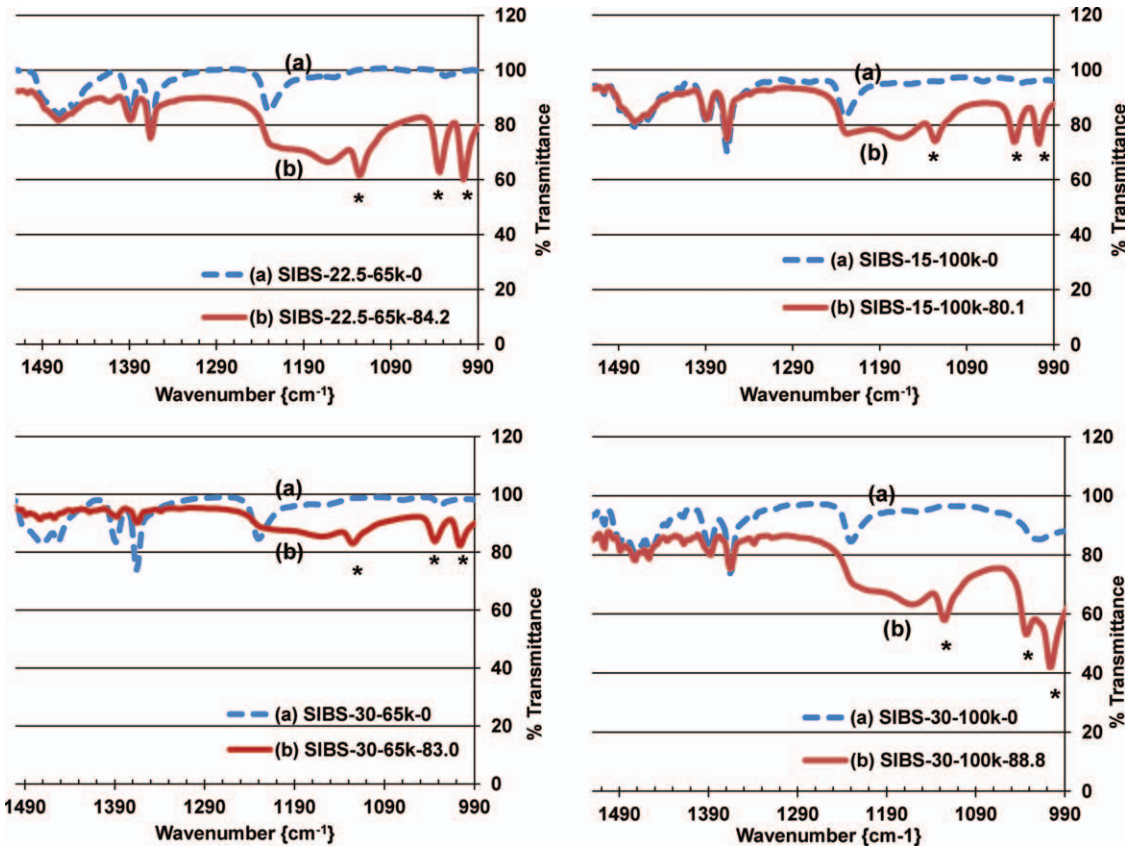

Figure 4. FTIR spectra for sulfonated and unsulfonated SIBS membranes. [Color figure can be viewed in the online issue, which is available at wileyonlinelibrary.com.]

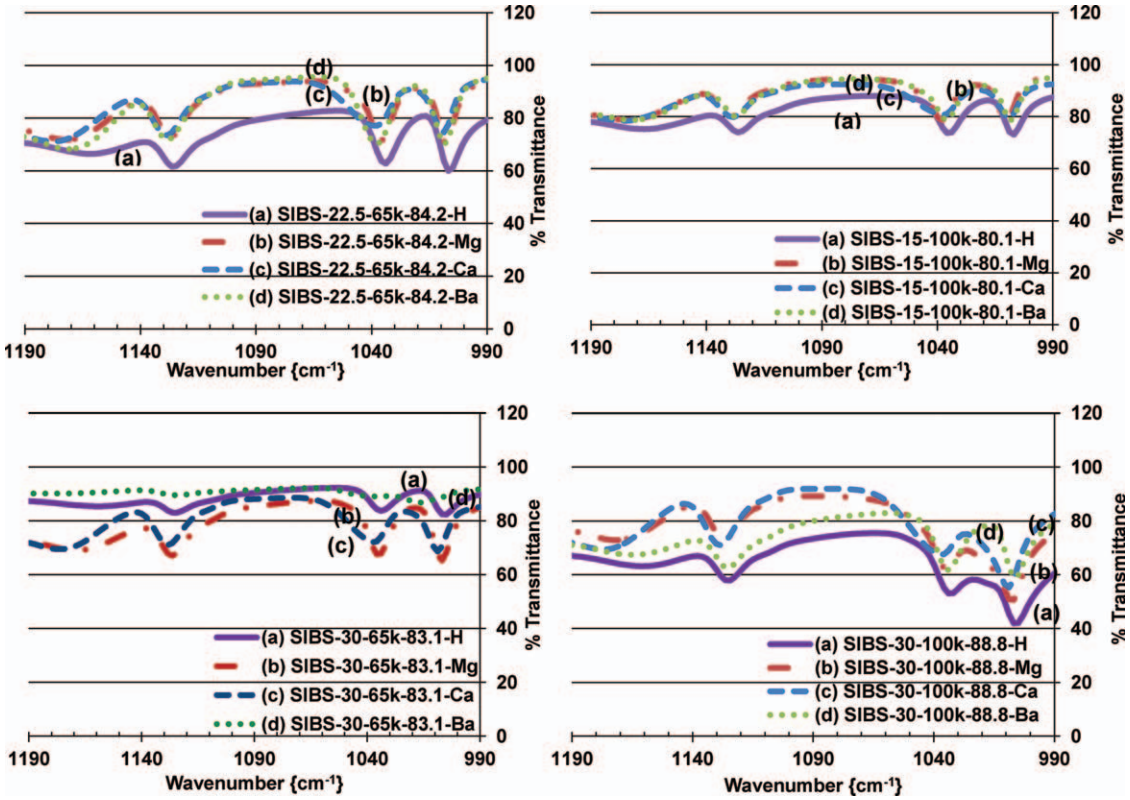

Figure 5. FTIR spectra for acid and cation-substituted sulfonated SIBS membranes. [Color figure can be viewed in the online issue, which is available at wileyonlinelibrary.com.]

other polymers. The second degradation temperature, the polymer backbone, was very similar for all polymers, regardless of M_n or PS weight fraction. In addition, the polymer backbone degradation temperature was higher (9–49°C) than in the unsulfonated polymers, perhaps as the sulfonated polymers have additional phase segregation on the interconnection of sulfonic groups. Sulfonation shifts polymer backbone degradation temperature to a consistent value of approximately 422 ± 3°C for all polymers studied regardless of the PS wt % or M_n.

The incorporation of cations provokes three major thermogravimetric effects: first, the sulfonic group degradation region disappears, as they are more thermally stable with the cations. Second, the polymer backbone degradation temperature is lower on the incorporation of the cations (compared to the acid form). Third, two new weight loss stages are observed for each cation at higher temperatures. For SIBS substituted with Ba^{+2}, it is observed that the polymer backbone degradation temperature has a reduction of approximately 10°C in comparison with SIBS without the cation. For SIBS substituted with Ca^{+2}, it is observed that (1) the polymer backbone degradation temperature decreases slightly with an increase in the % PS for M_n = 100,000 (similar trend observed in the unsulfonated polymers); (2) the additional degradation temperatures attributed to the incorporation of Ca^{+2} are the same regardless of the % PS or the M_n, except for SIBS-30-65k-83.1 that has a 14°C lower third and fourth degradations than the other polymers. For SIBS with Mg^{+2}, it is observed that the polymer backbone degradation temperature is the same regardless of the % PS or M_n, except for SIBS-30-65k-83.1 that has a 6°C higher degradation temperature. The incorporation of cations into SIBS suggests that they have two different coordination sites to the sulfonic groups and that the resulting structures could be very similar regardless of % PS or M_n for some polymers.

Small-Angle X-ray Scattering

SAXS profiles for the highly sulfonated membranes are presented in Figure 7. The highly sulfonated levels studied,

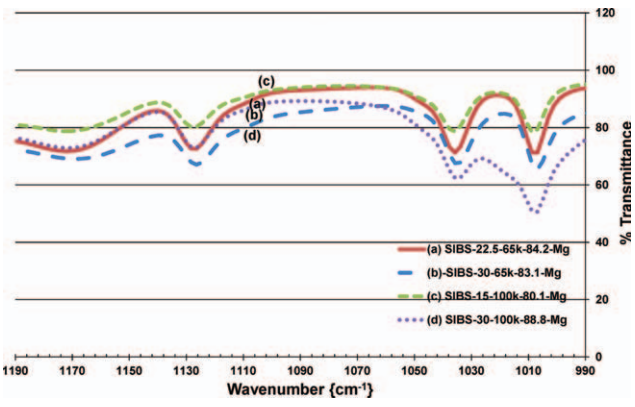

Figure 6. FTIR spectra for magnesium-substituted SIBS membranes. [Color figure can be viewed in the online issue, which is available at wileyonlinelibrary.com.]

Table II. SIBS Degradation Temperatures

Sample name	First degradation temperature (°C)	Second degradation temperature (°C)	Third degradation temperature (°C)	Fourth degradation temperature (°C)
SIBS-22.5-65k	N/A	400.8 ± 2.6	N/A	N/A
SIBS-30-65k	N/A	369.7 ± 1.2	N/A	N/A
SIBS-15-100k	N/A	416.1 ± 1.0	N/A	N/A
SIBS-30-100k	N/A	406.4 ± 0.6	N/A	N/A
SIBS-22.5-65k-84.1	265.3 ± 4.8	423.6 ± 2.3	N/A	N/A
SIBS-30-65k-83.1	256.8 ± 2.2	418.6 ± 2.1	N/A	N/A
SIBS-15-100k-81.7	278.4 ± 6.6	424.7 ± 1.5	N/A	N/A
SIBS-30-100k-76.0	261.5 ± 7.9	422.2 ± 1.9	N/A	N/A
SIBS-22.5-65k-84.1-Ba^{+2}	N/A	411.3 ± 2.0	491.5 ± 3.7	572.4 ± 5.5
SIBS-30-65k-83.1-Ba^{+2}	N/A	410.4 ± 1.2	484.0 ± 2.1	549.3 ± 3.3
SIBS-15-100k-81.7-Ba^{+2}	N/A	415.5 ± 0.9	481.6 ± 2.1	562.9 ± 19.0
SIBS-30-100k-76.0-Ba^{+2}	N/A	410.1 ± 3.2	478.8 ± 1.1	564.0 ± 2.5
SIBS-22.5-65k-84.1-Ca^{+2}	N/A	412.1 ± 0.4	498.8 ± 2.5	555.6 ± 2.0
SIBS-30-65k-83.1-Ca^{+2}	N/A	414.0 ± 1.3	484.0 ± 2.1	541.1 ± 1.4
SIBS-15-100k-81.7-Ca^{+2}	N/A	416.0 ± 0.4	498.5 ± 0.9	555.7 ± 2.8
SIBS-30-100k-76.0-Ca^{+2}	N/A	406.5 ± 2.2	494.6 ± 1.6	555.0 ± 2.2
SIBS-22.5-65k-84.1-Mg^{+2}	N/A	408.0 ± 3.8	504.7 ± 0.9	563.1 ± 3.5
SIBS-30-65k-83.1-Mg^{+2}	N/A	414.0 ± 3.6	500.3 ± 2.7	549.3 ± 2.1
SIBS-15-100k-81.7-Mg^{+2}	N/A	408.3 ± 4.8	503.0 ± 0.7	551.3 ± 6.8
SIBS-30-100k-76.0-Mg^{+2}	N/A	408.6 ± 2.7	497.9 ± 2.3	559.2 ± 3.3

although they have different degrees of crystallinity, they all show similar lamellar morphologies. Therefore, emphasis was placed on the ionomer peak (maxima in Figure 7). Bragg's Law was used to relate the wavelength of the X-rays with the spacing between the layers of atoms and the angle between the incident rays and the surface of the atoms (eq. 2):

$$\lambda = 2d \sin\theta \tag{2}$$

where λ is the wavelength, d is the distance between atoms, and θ is the angle. Combining Bragg's law with the scattering vector obtained from the SAXS plots, the interstitial distance between atoms can be calculated using eq. 3:

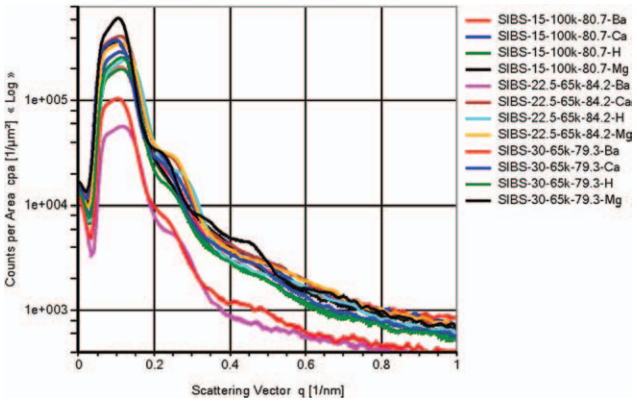

Figure 7. SAXS profiles for SIBS membranes. [Color figure can be viewed in the online issue, which is available at wileyonlinelibrary.com.]

$$d_{\text{Bragg}} = \frac{2\pi}{q_{\text{Bragg}}} \tag{3}$$

where d_{Bragg} is the distance between aligned atoms and q_{Bragg} is the scattering vector. Using the maxima observed in Figure 7 for the ionomer peak and eq. 3, the ionomer interstitial distance was calculated (Table III). It has been presented before that the insterstitial ionic distance increases with sulfonation.[5] Table III supports the increase in interstitial distance with overall sulfonation, but it also presents a slight increase (4.1–16.9%) in

Table III. Bragg's Interstitial Ionomer Distance

Polymer membrane	d_{Bragg} (nm)
SIBS-22.5-65k-84.2-H	50.6
SIBS-22.5-65k-84.2-Mg^{+2}	55.9
SIBS-22.5-65k-84.2-Ca^{+2}	57.6
SIBS-22.5-65k-84.2-Ba^{+2}	55.2
SIBS-30-65k-79.3-H	56.0
SIBS-30-65k-79.3-Mg^{+2}	60.7
SIBS-30-65k-79.3-Ca^{+2}	63.5
SIBS-30-65k-79.3-Ba^{+2}	59.1
SIBS-15-100k-80.7-H	55.4
SIBS-15-100k-80.7-Mg^{+2}	64.8
SIBS-15-100k-80.7-Ca^{+2}	57.7
SIBS-15-100k-80.7-Ba^{+2}	58.5

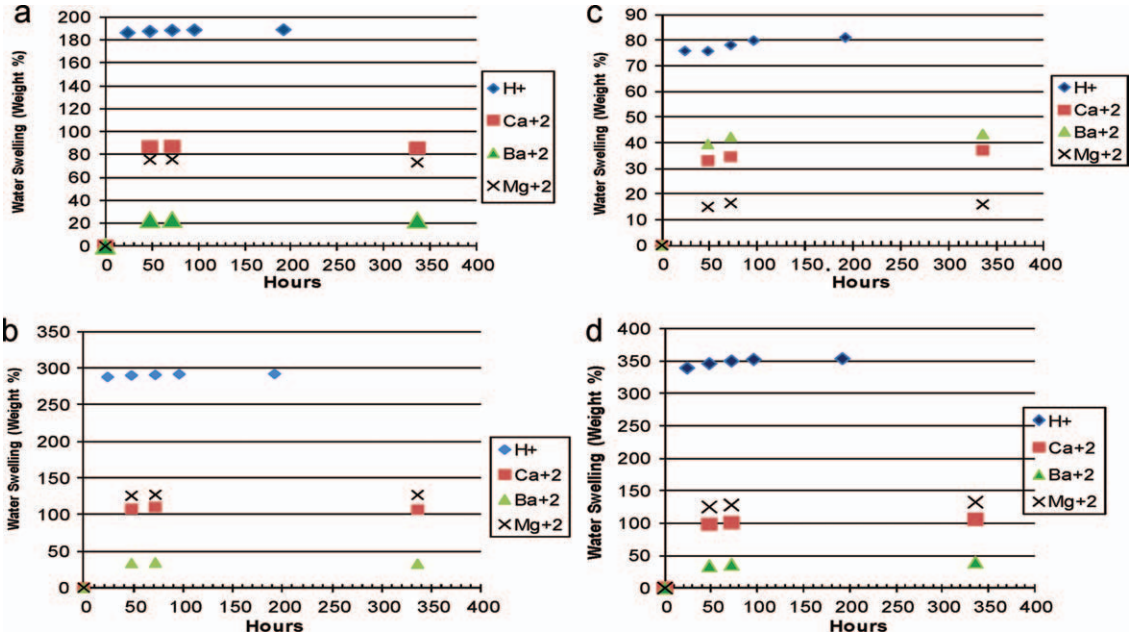

Figure 8. Water swelling experiments for SIBS membranes. [Color figure can be viewed in the online issue, which is available at wileyonlinelibrary.com.]

the interstitial ionic distance on cation substitution (recall the ionic radius for the cations studied is in the 0.16–0.22 nm range). No specific trends were observed for the cations studied.

Water Swelling

Water swelling is related to the amount of water absorbed by the sulfonic groups in the sulfonated polymers. Without sulfonation, all the polymers studied absorb zero water. On sulfonation, all polymers studied absorbed water with time reaching equilibrium after about 48 h; they were left for about 350 h to assure equilibrium (Figure 8). The highly sulfonated polymers absorbed as much as 350% (by weight) water. For all sulfonated polymers studied in their acid form, the amount of water swelling was proportional to the overall amount of sulfonic groups available (Figure 9).

The incorporation of cations significantly reduced the amount of water swelling (Figure 8); each cation reduced water swelling uniquely for each polymer. A possible explanation for the reduction in the amount of water swelling on the incorporation of the cations is that the cations compete with water for the lone electrons in the sulfonic groups. Although Ba^{+2} reduced the most swelling for most of the polymers, the trend was not consistent for all polymers studied. Table IV presents the moles of water absorbed per mole of sulfonic group for all the polymer membranes studied.

When the cation substitution was performed, only the magnesium substituted membrane followed a linear increase of water with sulfonation (Figure 10). During the cation-substitution process the pH of the solutions was monitored with time with the intention to quantify the number of cations in the membrane. The intention was also to quantify how the moles of cations competed with the moles of water absorbed for each sulfonic group. Unfortunately, the results were not reproducible, suggesting that pH might not be an accurate method for quantifying the number of cations in the membrane. Solid-state NMR is suggested to complete this analysis.

Vapor Permeability and Selectivity

The effect of toxic agents against the membranes was analyzed using DMMP effective permeability studies. DMMP showed lower permeabilities on the incorporation of cations. However, the incorporation of cations also decreased the vapor-phase permeability of water, perhaps as they interact with the sulfonic groups responsible for the water transport (Table V). These values, although similar to those obtained using linear and branched poly(styrene-isoprene-styrene), are higher in the effective water permeability and lower in the effective permeabililty of DMMP than in that study. In that study, isoprene was also sulfonated and loss some of its barrier properties. Perhaps, isobutylene is a better elastomer for barrier properties while the incorporation of cations provides additional selective control of

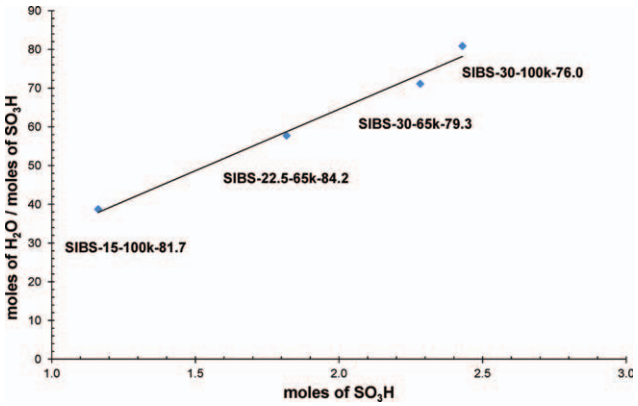

Figure 9. Water absorbed for all sulfonated membranes in their acid form. [Color figure can be viewed in the online issue, which is available at wileyonlinelibrary.com.]

Table IV. Water Absorbed for Polymer Membranes Studied

Polymer membrane	Moles of H_2O/moles of SO_3H	Polymer membrane	Moles of H_2O/moles of SO_3H
SIBS-22.5-65k-84.2-H	57.7	SIBS-15-100k-80.7-H	38.7
SIBS-22.5-65k-84.2-Mg^{+2}	22.3	SIBS-15-100k-80.7-Mg^{+2}	7.6
SIBS-22.5-65k-84.2-Ca^{+2}	26.1	SIBS-15-100k-80.7-Ca^{+2}	17.7
SIBS-22.5-65k-84.2-Ba^{+2}	6.9	SIBS-15-100k-80.7-Ba^{+2}	20.7
SIBS-30-65k-79.3-H	71.1	SIBS-30-100k-79.3-H	80.9
SIBS-30-65k-79.3-Mg^{+2}	30.8	SIBS-30-100k-79.3-Mg^{+2}	30.3
SIBS-30-65k-79.3-Ca^{+2}	26.0	SIBS-30-100k-79.3-Ca^{+2}	24.2
SIBS-30-65k-79.3-Ba^{+2}	8.0	SIBS-30-100k-79.3-Ba^{+2}	9.1

the transport through the ionic nanochannels. To get a more accurate measure of the separation efficiency, selectivity calculations were made using eq. 4:

$$\alpha = \frac{P_{\text{eff(water)}}}{P_{\text{eff(DMMP)}}} \quad (4)$$

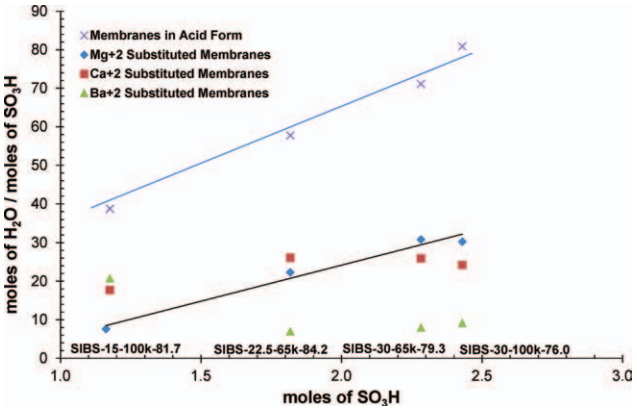

Figure 10. Water absorbed for all membranes studied. [Color figure can be viewed in the online issue, which is available at wileyonlinelibrary.com.]

Results in Figure 11 and Table V show that all cations improved the selectivity, but some cations improved the selectivity of the polymer membrane up to 34. One possible explanation for the difference in selectivities of Figure 11 could be attributed to the metal coordination for each polymer/sulfonation level and the free electrons available for transport through the ionomer nanochannels. For this to be better understood, a more in-depth study of the metal coordination using solid-state NMR is suggested.

CONCLUSIONS

In this study, linear poly(styrene-isobutylene-styrene) of different PS weight fraction and M_n were studied as a function of sulfonation and cation substitution. Variations in PS weight fraction and size (M_n) change the interstitial distance of the ionic group within the polymer (ionomer), but overall

Table V. Vapor Permeabilities of DMMP and Water at 308 K

Sample Name	P_{eff} (Water) × 10^3 (cm^2/s)	P_{eff} (DMMP) × 10^3(cm^2/s)	Selectivity($P_{eff\text{-}Water}/P_{eff\text{-}DMMP}$)
SIBS-22.5-65k-84.2	6.1	1.7	3.6
SIBS-22.5-65k-84.2-Mg^{+2}	3.8	0.6	5.9
SIBS-22.5-65k-84.2-Ca^{+2}	6.3	0.4	14.8
SIBS-22.5-65k-84.2-Ba^{+2}	1.7	0.1	23.0
SIBS-30-65k-79.3	3.2	2.2	1.4
SIBS-30-65k-79.3-Mg^{+2}	5.8	0.6	9.1
SIBS-30-65k-79.3-Ca^{+2}	4.8	1.1	4.5
SIBS-30-65k-79.3-Ba^{+2}	3.2	0.1	30.1
SIBS-15-100k-80.7	1.1	0.4	2.7
SIBS-15-100k-80.7-Mg^{+2}	1.4	0.3	4.3
SIBS-15-100k-80.7-Ca^{+2}	3.0	0.1	27.9
SIBS-15-100k-80.7-Ba^{+2}	0.6	0.1	9.0
SIBS-30-100k-84.4	0.7	1.0	0.7
SIBS-30-100k-84.4-Mg^{+2}	5.5	0.8	6.4
SIBS-30-100k-84.4-Ca^{+2}	5.6	0.6	8.8
SIBS-30-100k-84.4-Ba^{+2}	3.6	0.1	34.4

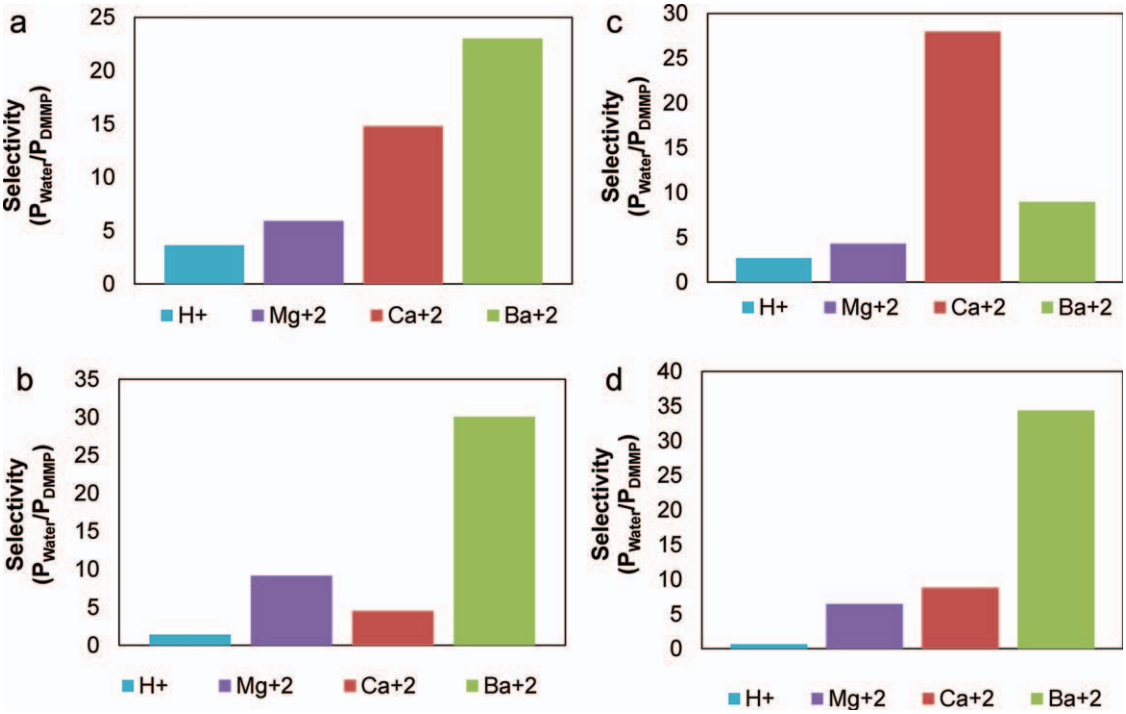

Figure 11. Selectivity (water/DMMP vapor effective permeabilities) at 308K for (a) SIBS-22.5-65k-84.2 (b) SIBS-30-65k-79.3 (c) SIBS-15-100k-80.7 (d) SIBS-30-100k-84.4. [Color figure can be viewed in the online issue, which is available at wileyonlinelibrary.com.]

sulfonation remains the most significant contributor to the interstitial distance. The incorporation of cations creates unique thermogravimetric transitions for each cation, but similar for all polymers studied. However, the selectivity of the membranes is unique for each polymer/cation, suggesting that the electronic environment inside the ionic nanochannel is affected and partly responsible for the transport through the membranes.

ACKNOWLEDGMENTS

This material is based upon work supported by the U. S. Army Research Laboratory and the U. S. Army Research Office under grant numbers W911-NF-07-10244 and W911-NF-10-0486. The authors would also like to acknowledge the support of Prof. Danilo C. Pozzo, of the University of Washington, where the SAXS experiments were conducted (NSF DMR 0817622). Finally, the authors would also like to acknowledge the help and support in the laboratory of: Alexandra González, Boris Rentería, and Sonia L. Avilés.

REFERENCES

1. Lee, S.; Obendorf, S. K. *J. Appl. Polym. Sci.* **2006,** *102*, 3430.
2. Wang, D.; Liu, N.; Xu, W.; Sun, G. *J. Phys. Chem.* **2011,** *115*, 6825.
3. Elabd, Y. A.; Napadensky, G. *Polymer* **2004,** *45*, 3037.
4. Elabd, Y. A.; Napadensky, G.; Sloan, J. M.; Crawford, D. M.; Walker, C. W. *J. Membr. Sci.* **2003,** *217*, 227.
5. Elabd, Y. A.; Napadensky, G.; Walker, C. W.; Winey, K. I. *Macromolecules* **2006,** *39*, 399.
6. Joseph, J. G. *Polym. Adv. Technol.* **2007,** *18*, 785.
7. Carretta, N.; Tricoli, V.; Picchioni, F. *J. Membr. Sci.* **2000,** *166*, 189.
8. Raghu, P.; Nere, C. K.; Jagtap, R. N. *J. Appl. Polym. Sci.* **2003,** *88*, 266.
9. Liu, B.; Wang, G.; Hu, W.; Chen, C.; Jiang, Z.; Zhang, W.; Wu, Z.; Wei, Y. *J. Polym. Sci. Part A: Polym. Chem.* **2002,** *40*, 3392.
10. Liu, B.; Hu, W.; Chen, C.; Jiang, Z.; Zhang, W.; Wu, Z.; Matsumoto, T. *Polymer* **2010,** *45*, 3241.
11. Zhao, Y.; Yin, J. *Eur. Polym. J.* **2010,** *46*, 592.
12. Dimitrova, G. P.; Baradie, B.; Foscallo, D.; Poinsignon, C.; Sanchez, J. Y. *J. Membr. Sci.* **2001,** *185*, 59.
13. Yang, Y.; Shi, Z.; Holdcroft, S. *Macromolecules* **2004,** *37*, 1678.
14. Fang, J. H.; Guo, X. X.; Harada, S.; Watari, T.; Tanaka, K.; Kita, H., et al *Macromolecules* **2002,** *35*, 9022.
15. Asano, N.; Aoki, M.; Suzuki, S.; Miyatake, K.; Uchida, H.; Watanabe, M. *J. Am. Chem. Soc.* **2006,** *128*, 1762.
16. Miyatek, K.; Yasuda, T.; Hirai, M.; Nanasawa, M.; Watanabe, M. *J. Polym. Sci. Part A: Polym. Chem.* **2007,** *45*, 157.
17. Chen, S.; Yin, Y.; Kita, H.; Okamoto, K. I. *J. Polym. Sci. Part A: Polym. Chem.* **2007,** *45*, 2797.
18. Zare, P.; Stojanovic, A.; Herbst, F.; Akbarzadeh, J.; Peterlik, H.; Binder, W. *Macromolecules* **2012,** *45*, 2074.
19. Cheng, S.; Beyer, F. L.; Mather, B. D.; Moore, R. B.; Long, T. E. *Macromolecules* **2011,** *44*, 6509.

20. Avilés, S.; Suleiman, D. *J. Membr. Sci.* **2010,** *362*, 471.

21. Kim, Y. M.; Choi, S. H.; Lee, H. C.; Hong, M. Z.; Kim, K.; Lee, H. I. *Electrochim. Acta.* **2004,** *49*, 4787.

22. Tripathy, B. P.; Shahi, V. K. *Prog. Polym. Sci.* **2011,** *36*, 945.

23. Amjadi, M.; Rowshanzamir, S.; Peighambardoust, S. J.; Hossein, M. G.; Eikani, M. H. *J. Hydrogen Energy* **2010,** *35*, 9252.

24. Saritha, A.; Joseph, K.; Boudenne, A.; Thomas, S. *Polym. Compos.* **2011,** *32*, 1681.

25. Ghosal, K.; Freeman, B. D. *Polym. Adv. Technol.* **1994,** *5*, 673.

26. Suleiman, D.; Napadensky, E.; Sloan, J. M.; Crawford, D. M. *Thermochim. Acta.* **2005,** *430*, 149.

27. Suleiman, D.; Sloan, J. M.; Crawford, D. M. *Thermochim. Acta.* **2007,** *460*, 35.